Supplementary Material for CrystEngComm

Supplementary Materials

for

Hydrothermal Chemistry of Vanadium Oxides with Aromatic di- and tri-Phosphonates in the Presence of Secondary Metal-Organic Subunits

Paul DeBurgomaster, Wayne Ouellette, Hongxue Liu, Charles J. O'Connor and Jon Zubieta

I. ORTEP Figures: S1 to S21.

II. Magnetic Susceptibility Plots: S22 to S36.

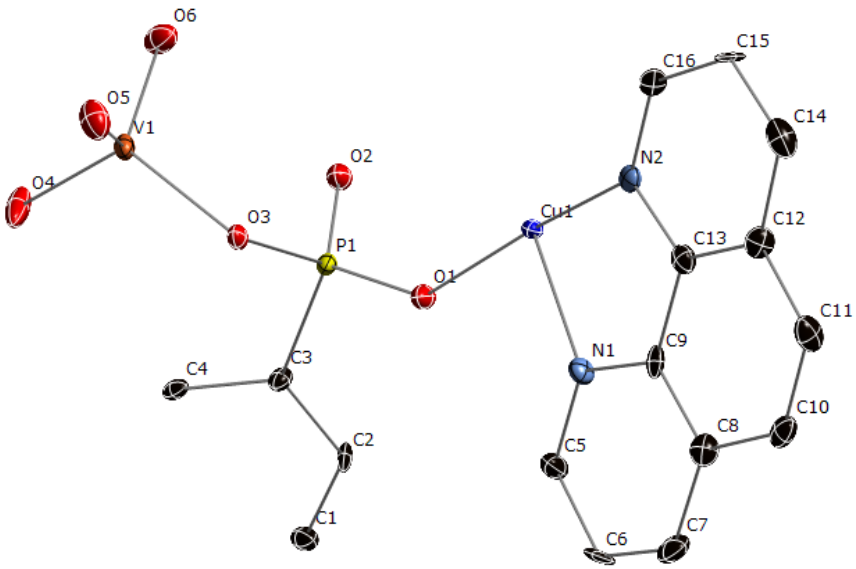

Figure S1. ORTEP plot of the asymmetric unit of compound **1**, showing the 50% thermal ellipsoids.

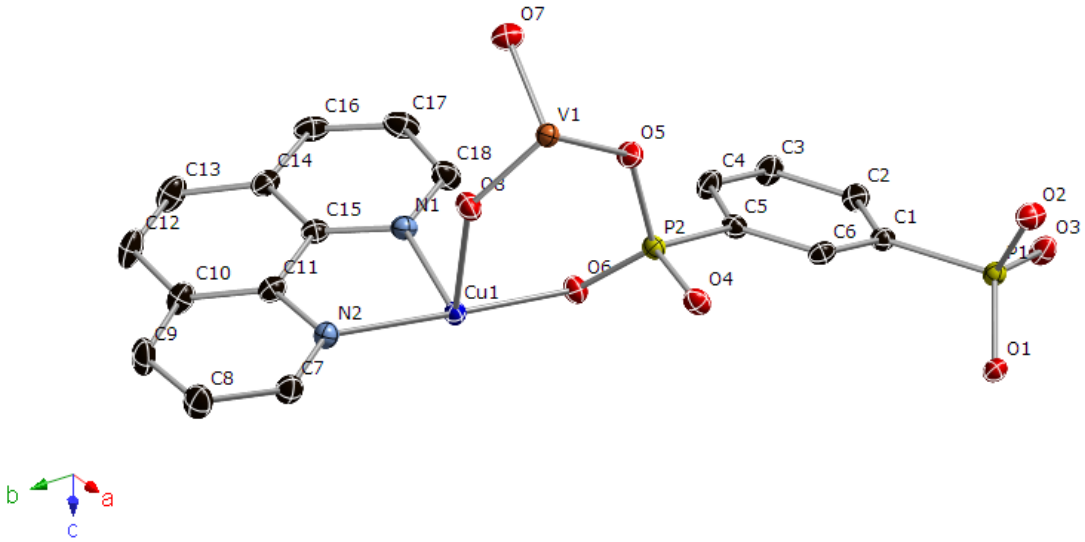

Figure S2. ORTEP plot of the asymmetric unit of compound **2**, showing the 50% thermal ellipsoids.

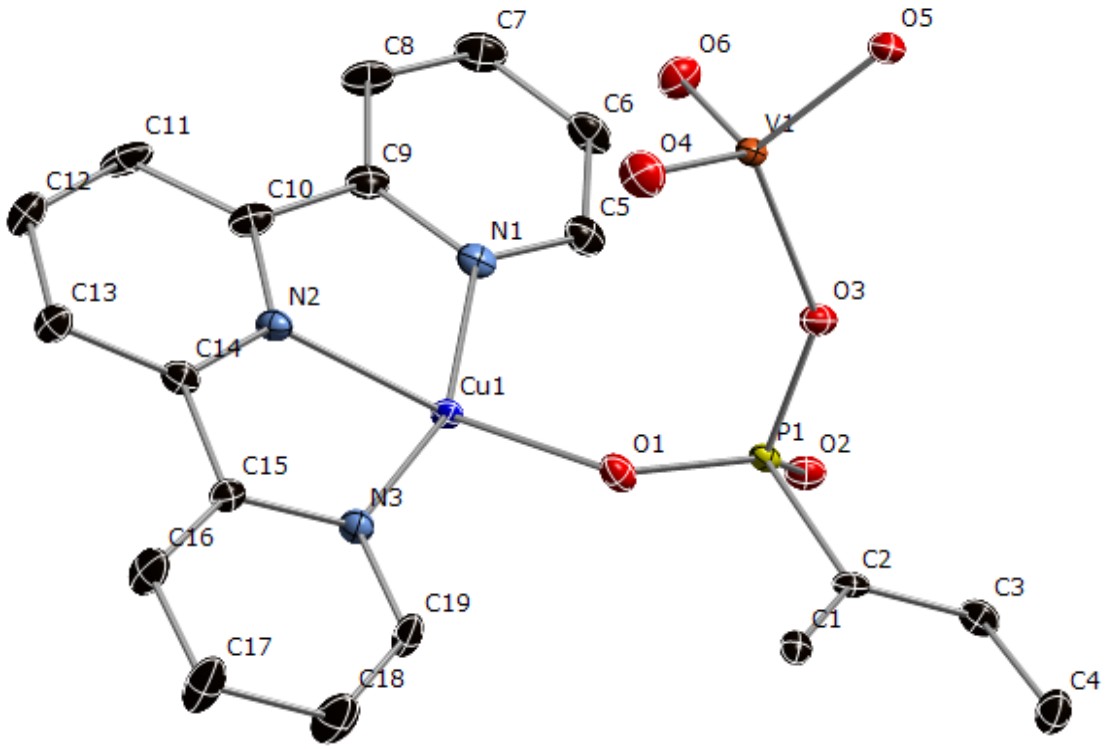

Figure S3. ORTEP plot of the asymmetric unit of compound **3**, showing the 50% thermal ellipsoids.

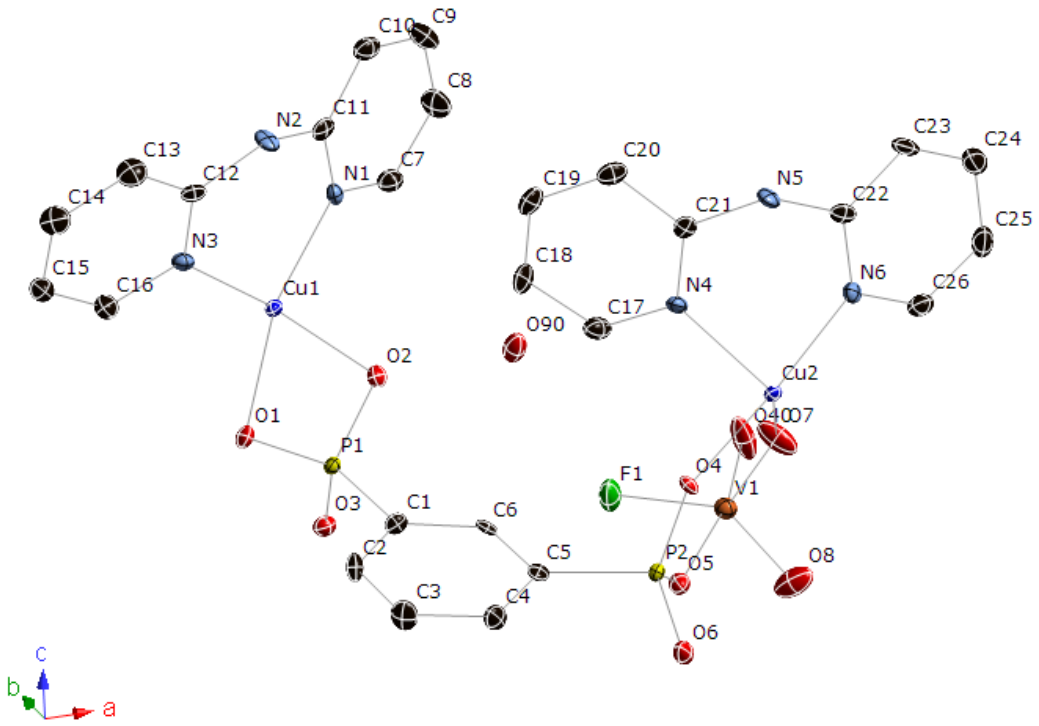

Figure S4. ORTEP plot of the asymmetric unit of compound **4**, showing the 50% thermal ellipsoids.

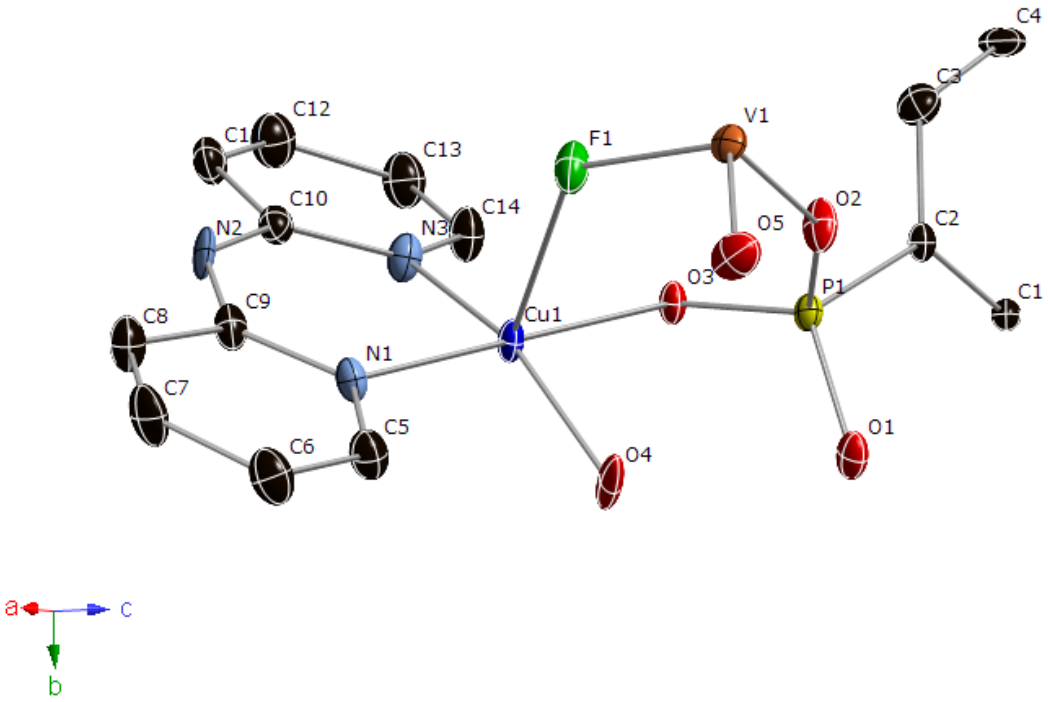

Figure S5. ORTEP plot of the asymmetric unit of compound **5**, showing the 50% thermal ellipsoids.

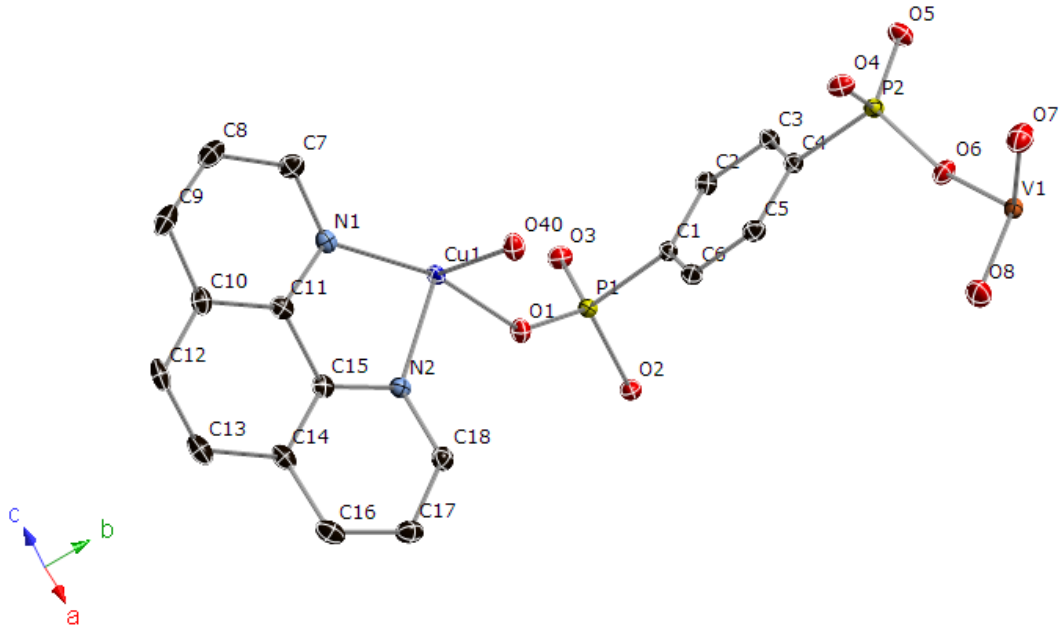

Figure S6. ORTEP plot of the asymmetric unit of compound **6**, showing the 50% thermal ellipsoids.

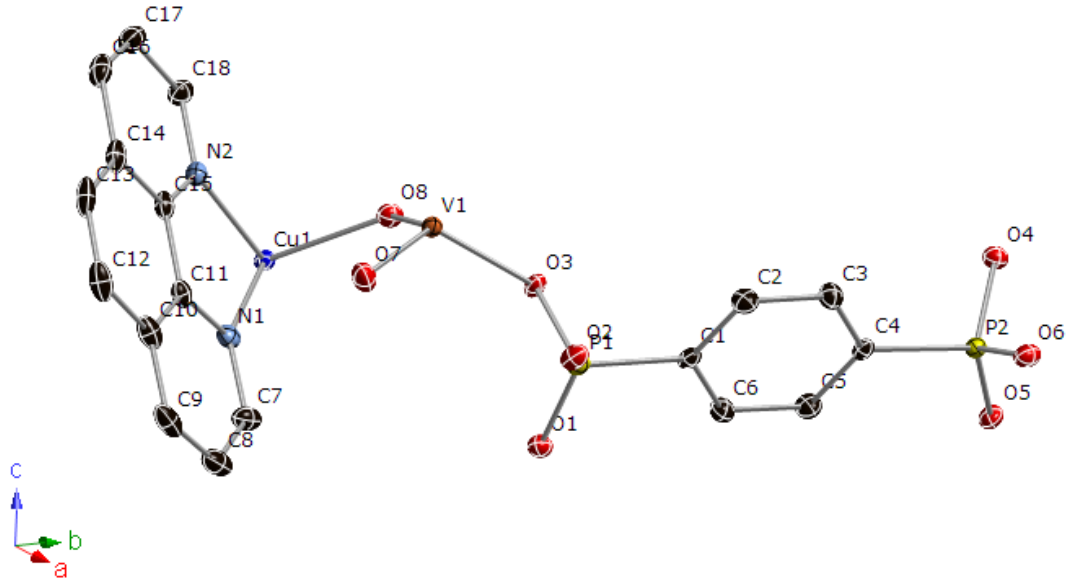

Figure S7. ORTEP plot of the asymmetric unit of compound **7a**, showing the 50% thermal ellipsoids.

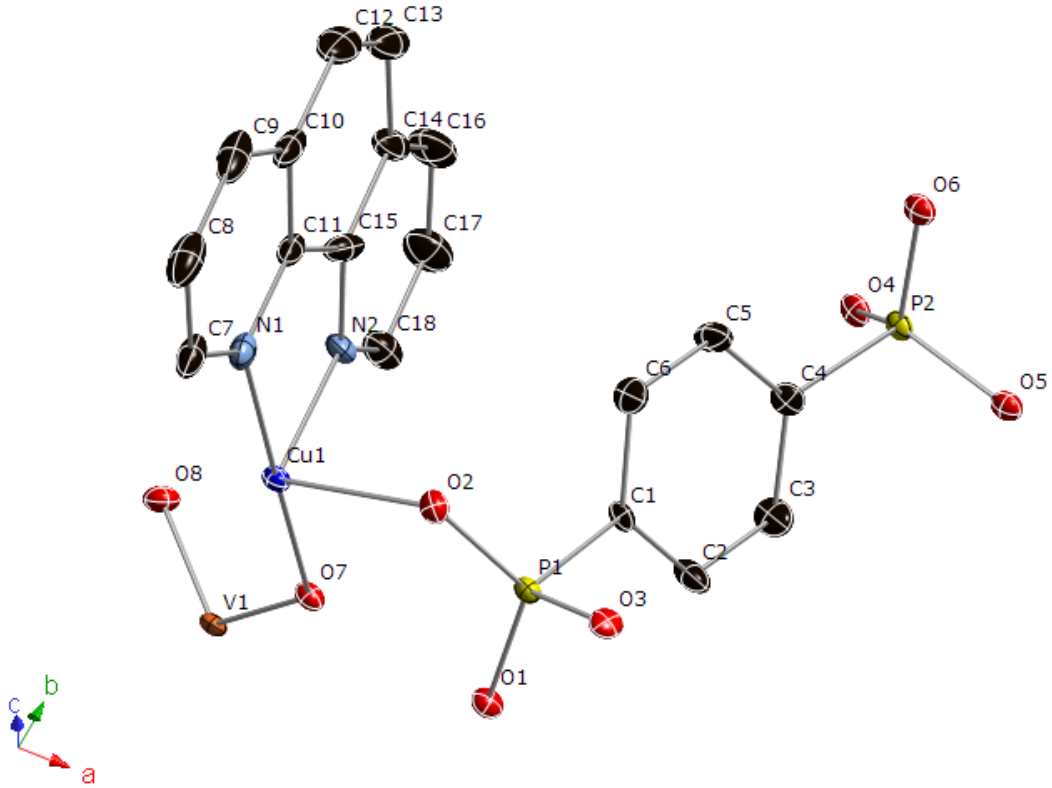

Figure S8. ORTEP plot of the asymmetric unit of compound **7b**, showing the 50% thermal ellipsoids.

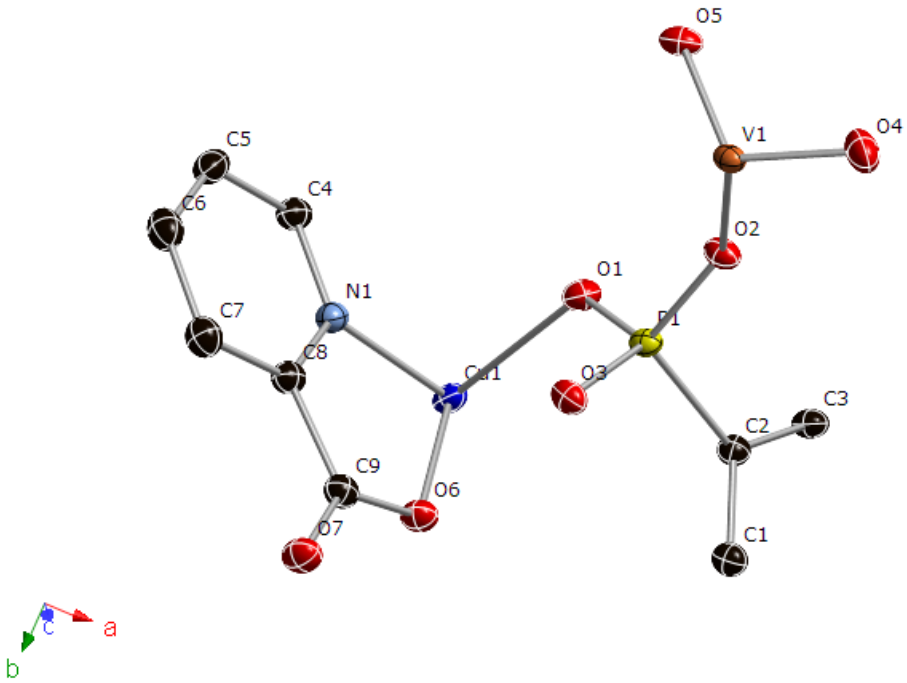

Figure S9. ORTEP plot of the asymmetric unit of compound **8**, showing the 50% thermal ellipsoids.

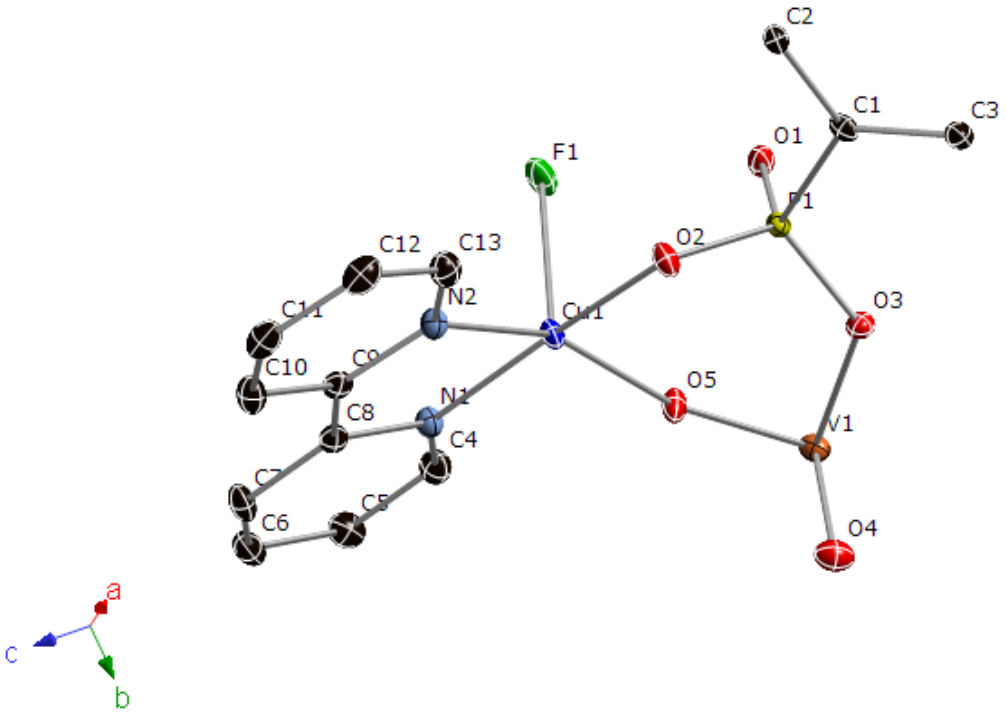

Figure S10. ORTEP plot of the asymmetric unit of compound **9**, showing the 50% thermal ellipsoids.

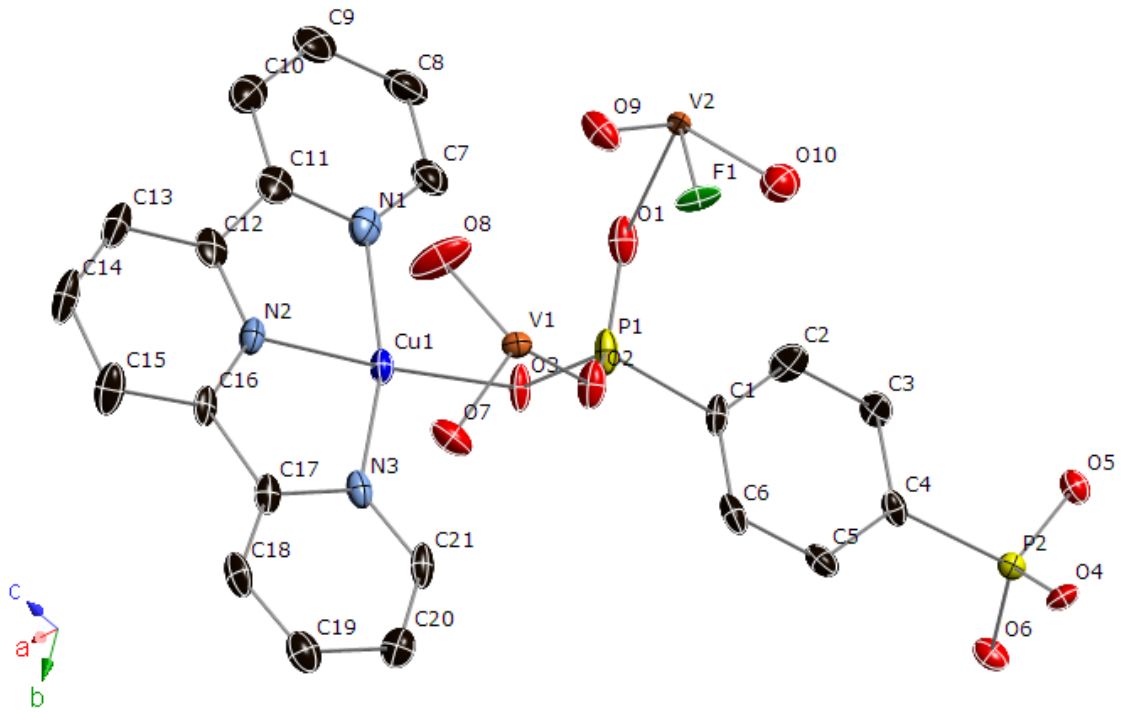

Figure S11. ORTEP plot of the asymmetric unit of compound **10**, showing the 50% thermal ellipsoids.

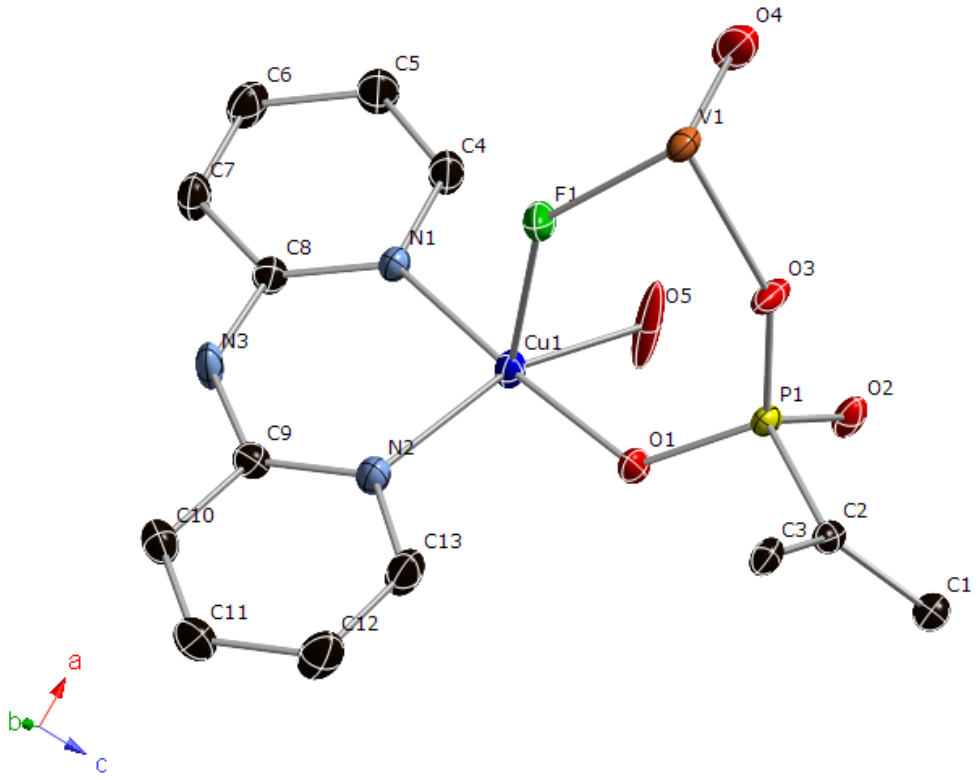

Figure S12. ORTEP plot of the asymmetric unit of compound **11**, showing the 50% thermal ellipsoids.

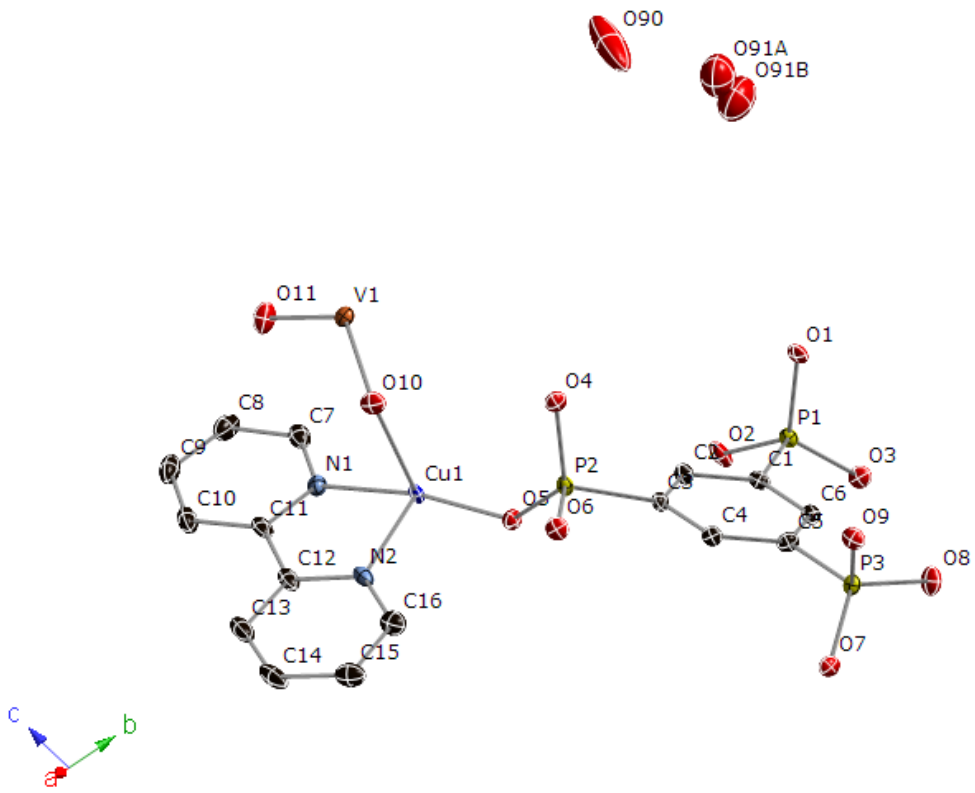

Figure S13. ORTEP plot of the asymmetric unit of compound **12**, showing the 50% thermal ellipsoids.

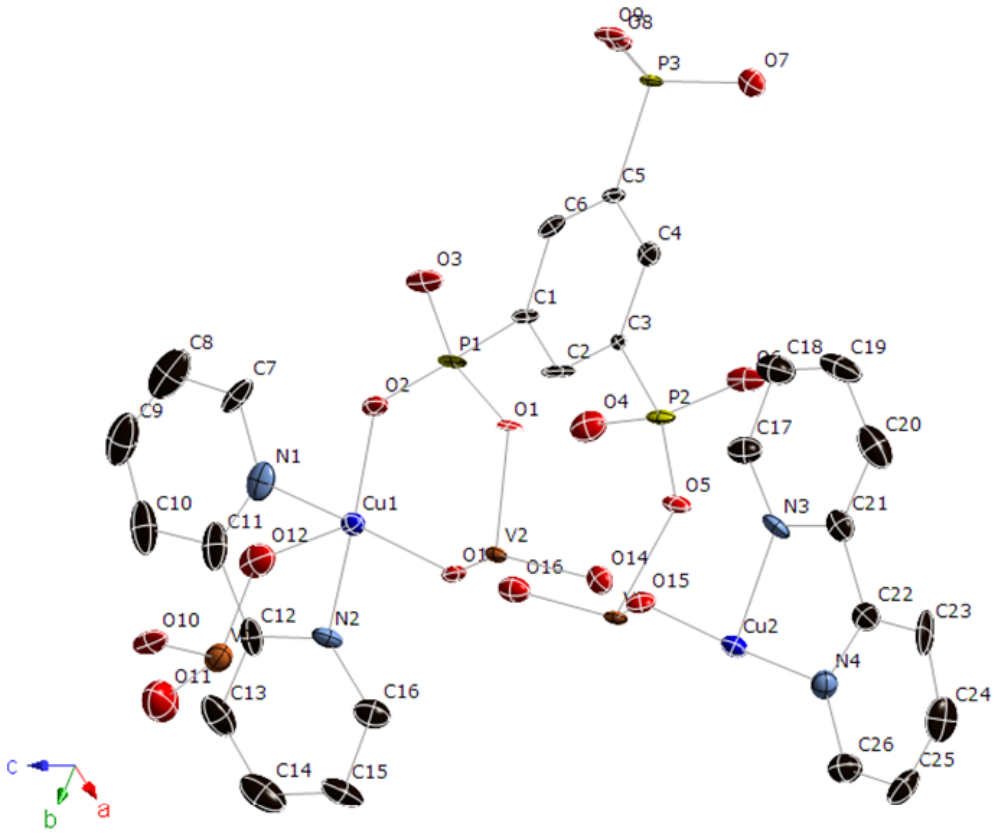

Figure S14. ORTEP plot of the asymmetric unit of compound **13**, showing the 50% thermal ellipsoids.

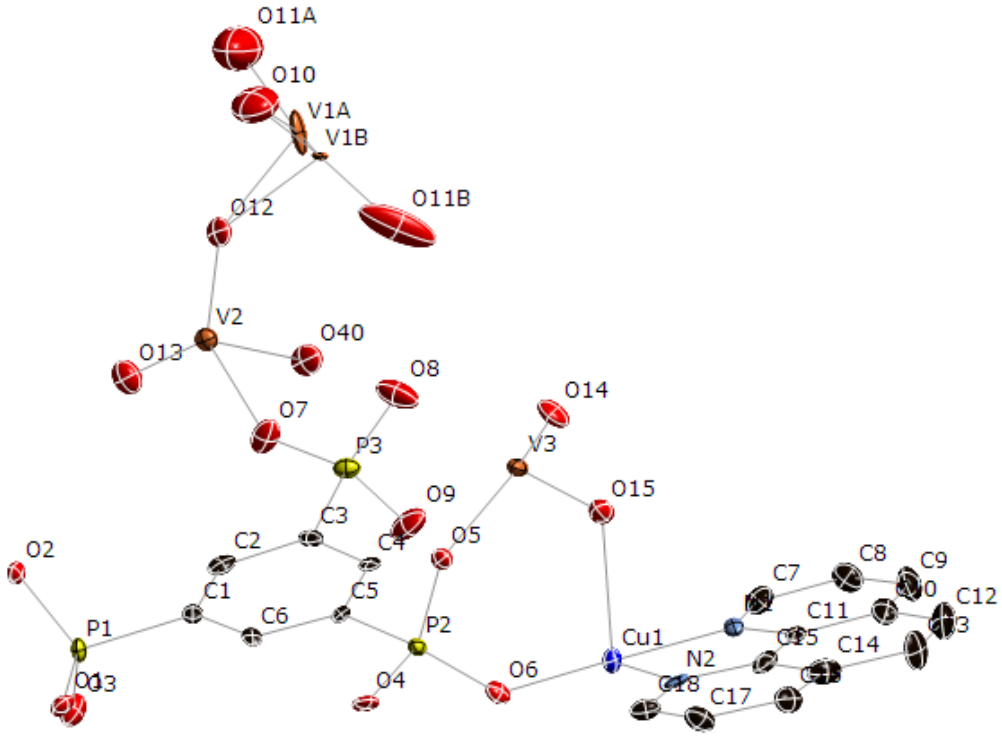

Figure S15. ORTEP plot of the asymmetric unit of compound **14**, showing the 50% thermal ellipsoids.

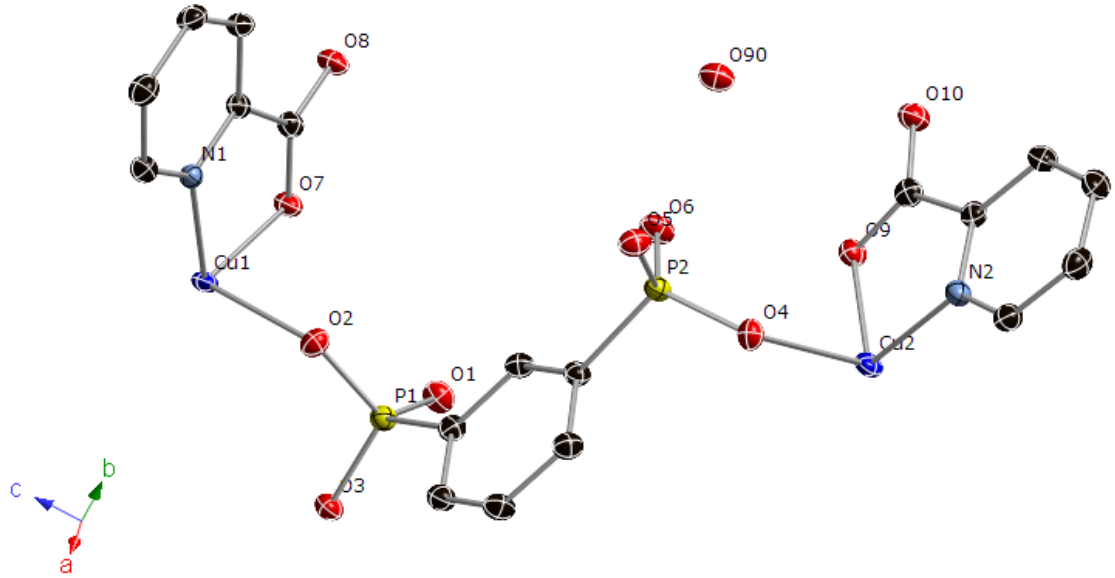

Figure S16. ORTEP plot of the asymmetric unit of compound **15**, showing the 50% thermal ellipsoids.

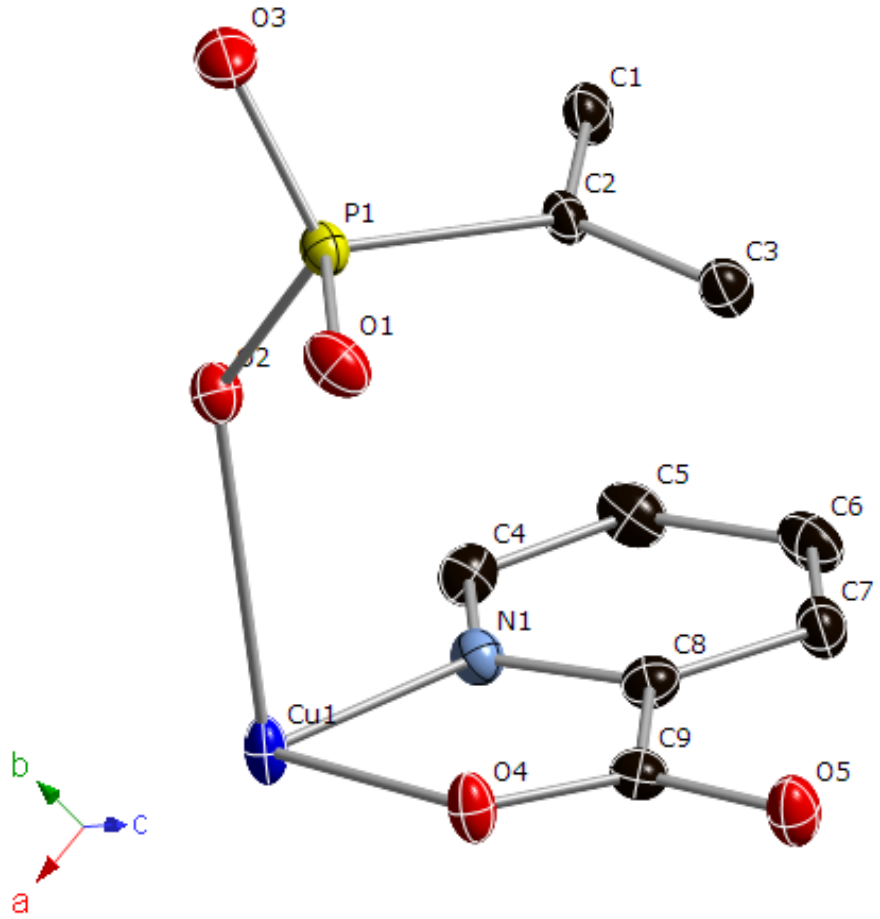

Figure S17. ORTEP plot of the asymmetric unit of compound **16**, showing the 50% thermal ellipsoids.

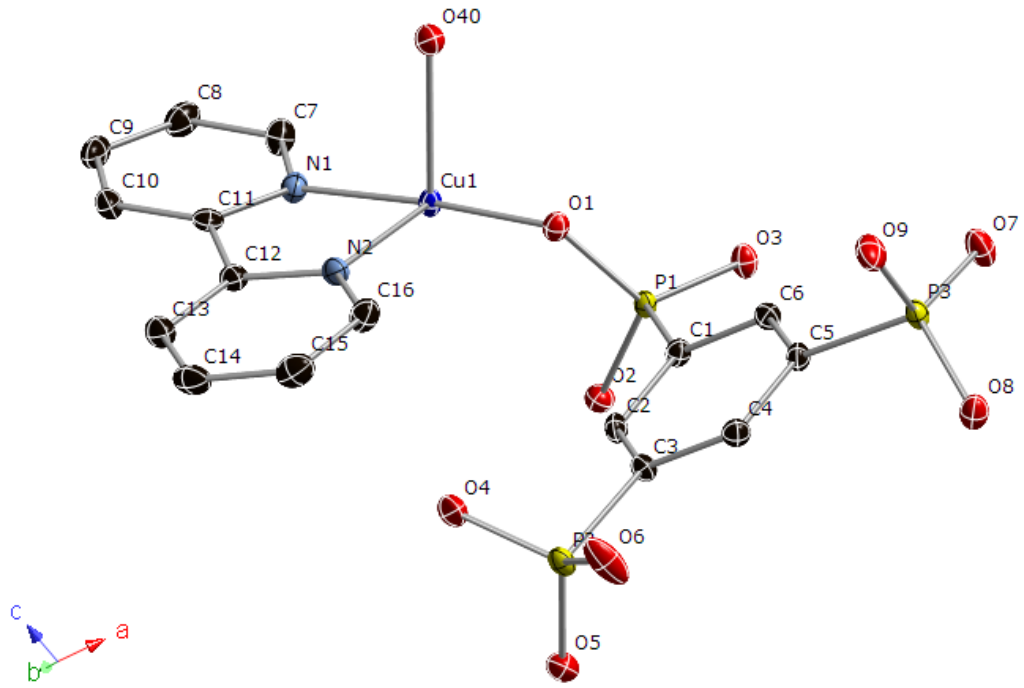

Figure S18. ORTEP plot of the asymmetric unit of compound **17**, showing the 50% thermal ellipsoids.

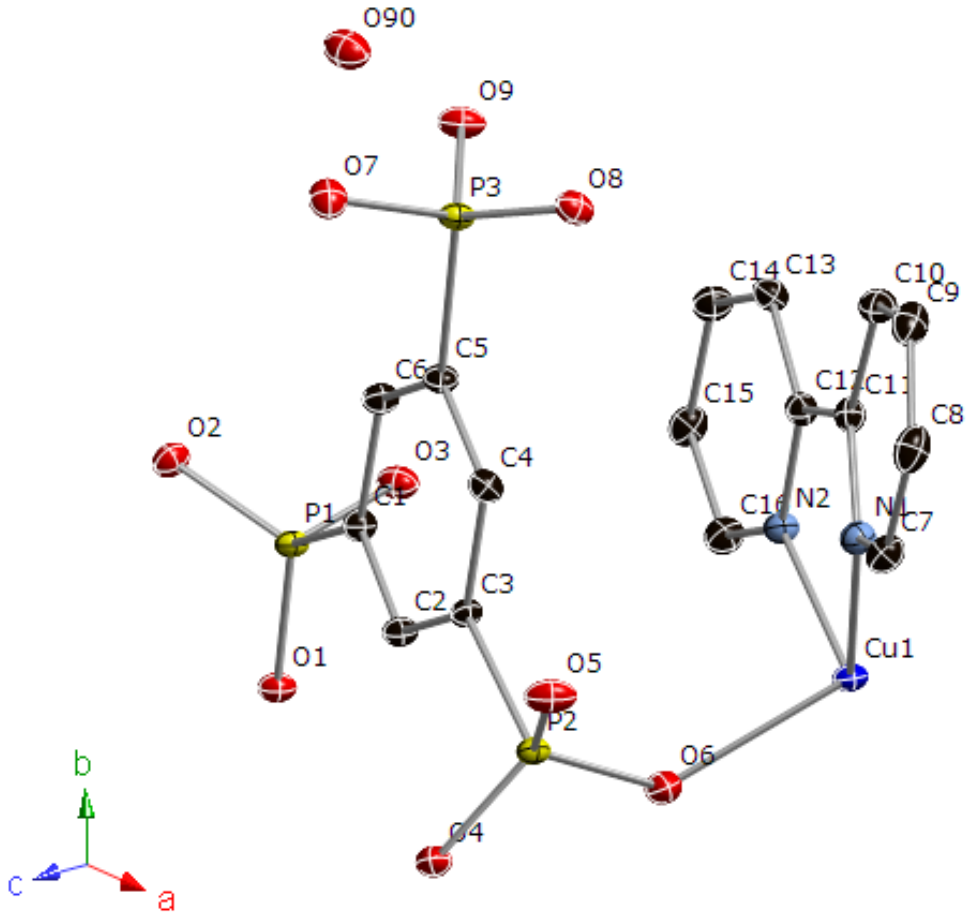

Figure S19. ORTEP plot of the asymmetric unit of compound **18**, showing the 50% thermal ellipsoids.

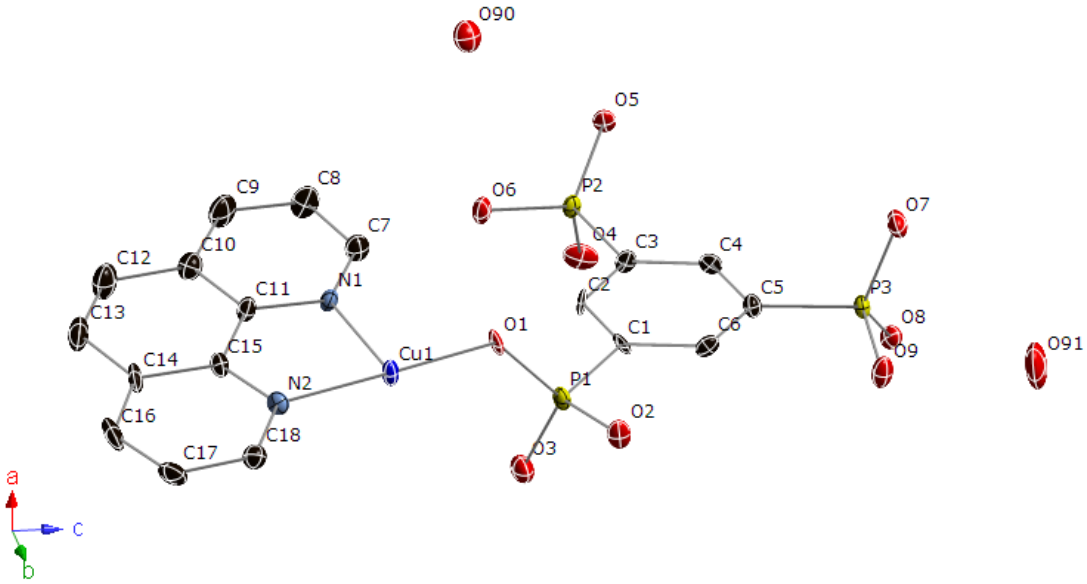

Figure S20. ORTEP plot of the asymmetric unit of compound **19**, showing the 50% thermal ellipsoids.

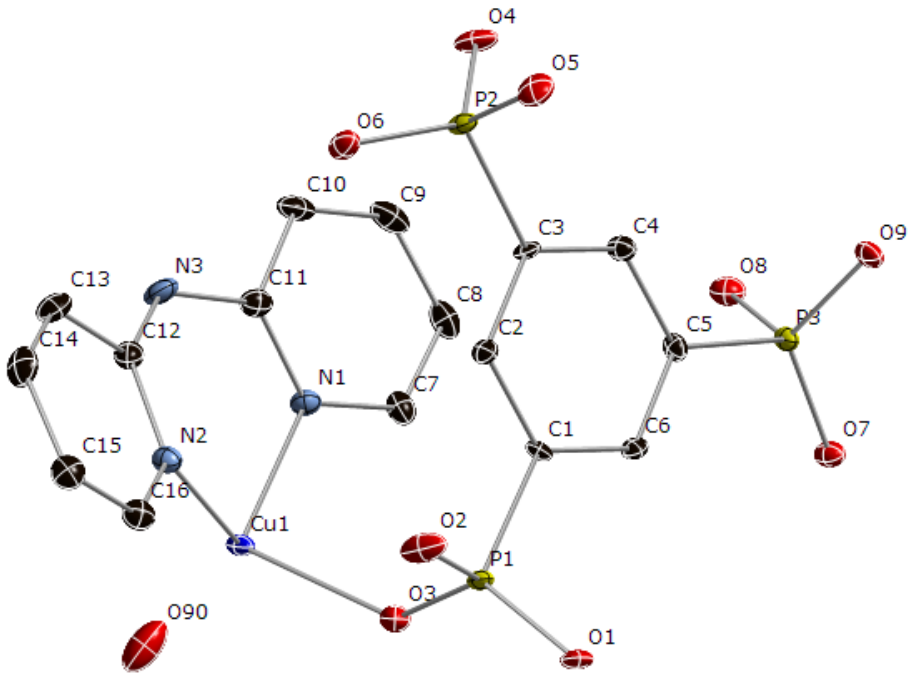

Figure S21. ORTEP plot of the asymmetric unit of compound **20**, showing the 50% thermal ellipsoids.

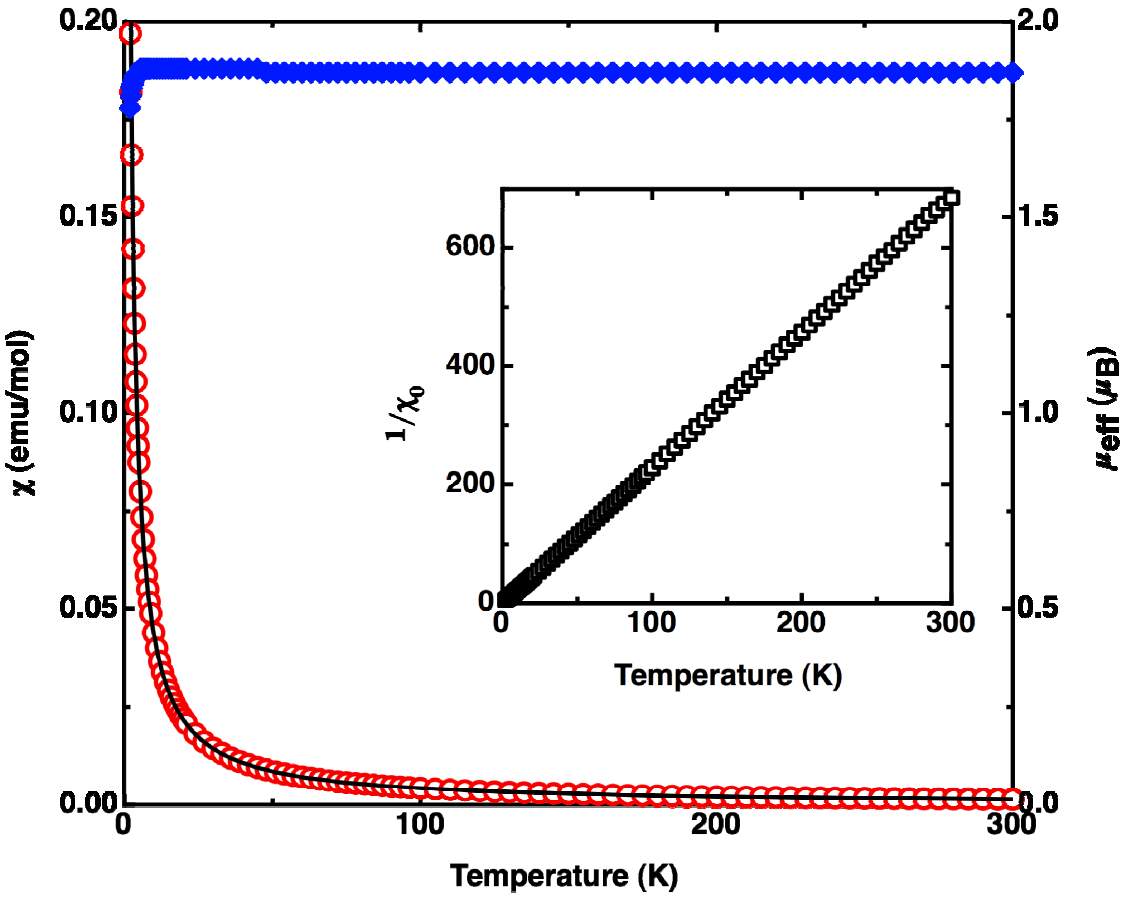

Figure S22. The temperature dependence of the magnetic susceptibility χ (red circles) and of the effective magnetic moment μ_{eff} (blue diamonds) of compound **2** in the 2-300 K temperature range. The inset shows the temperature dependence of the inverse susceptibility $1/\chi_0$.

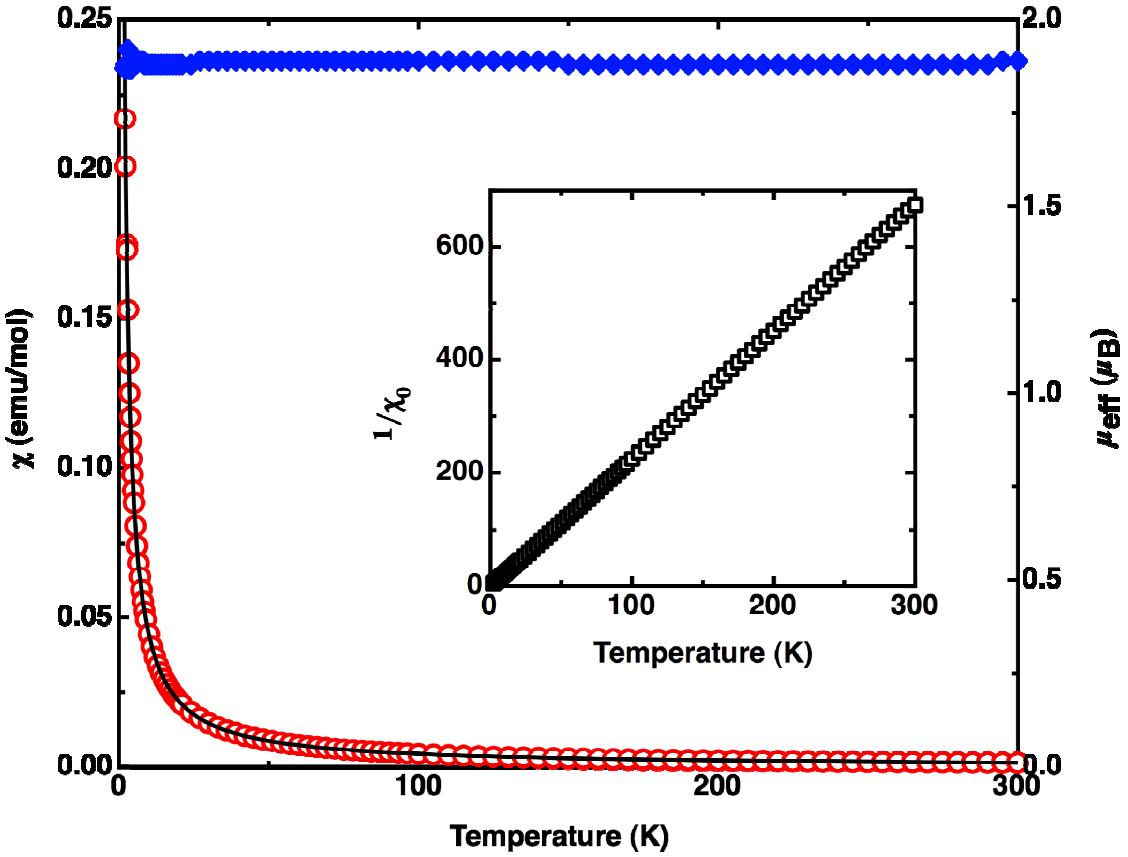

Figure S23. The temperature dependence of the magnetic susceptibility χ (red circles) and of the effective magnetic moment μ_{eff} (blue diamonds) of compound **3** in the 2-300 K temperature range. The inset shows the temperature dependence of the inverse susceptibility $1/\chi_0$.

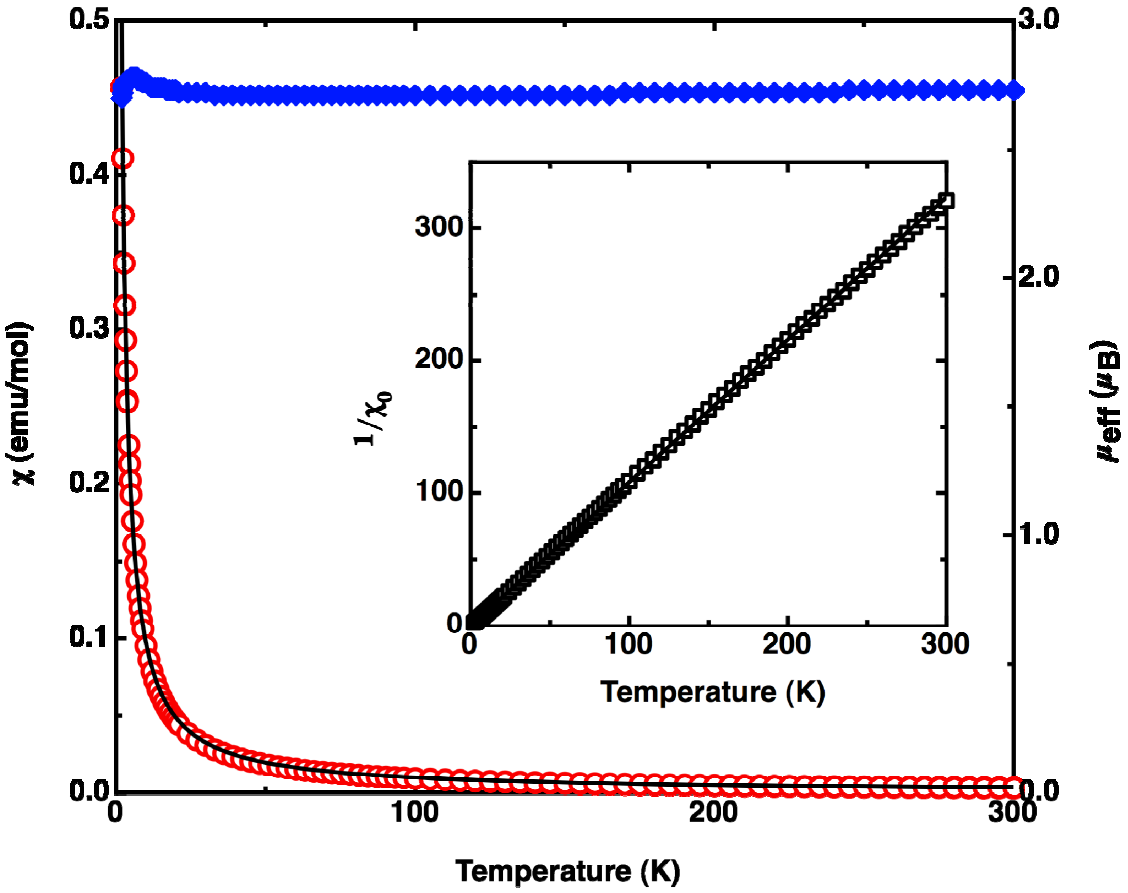

Figure S24. The temperature dependence of the magnetic susceptibility χ (red circles) and of the effective magnetic moment μ_{eff} (blue diamonds) of compound **4** in the 2-300 K temperature range. The inset shows the temperature dependence of the inverse susceptibility $1/\chi_0$.

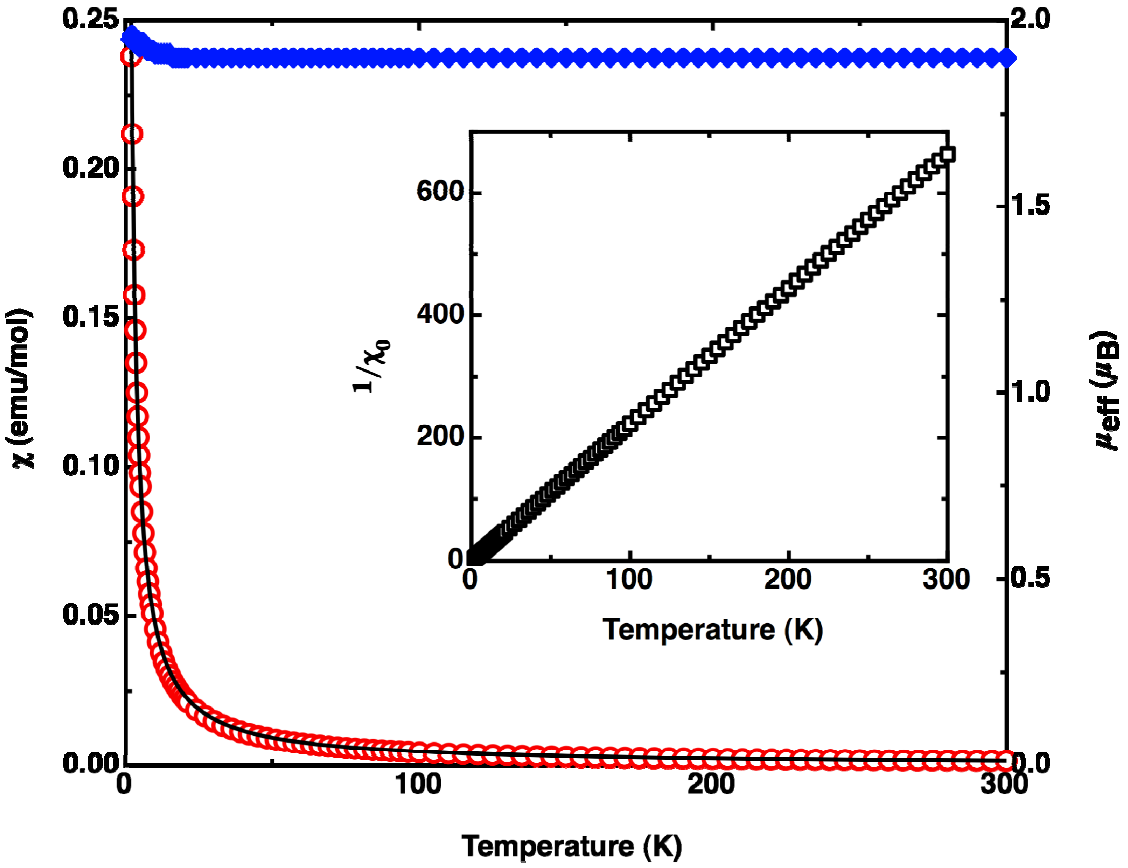

Figure S25. The temperature dependence of the magnetic susceptibility χ (red circles) and of the effective magnetic moment μ_{eff} (blue diamonds) of compound **5** in the 2-300 K temperature range. The inset shows the temperature dependence of the inverse susceptibility $1/\chi_0$.

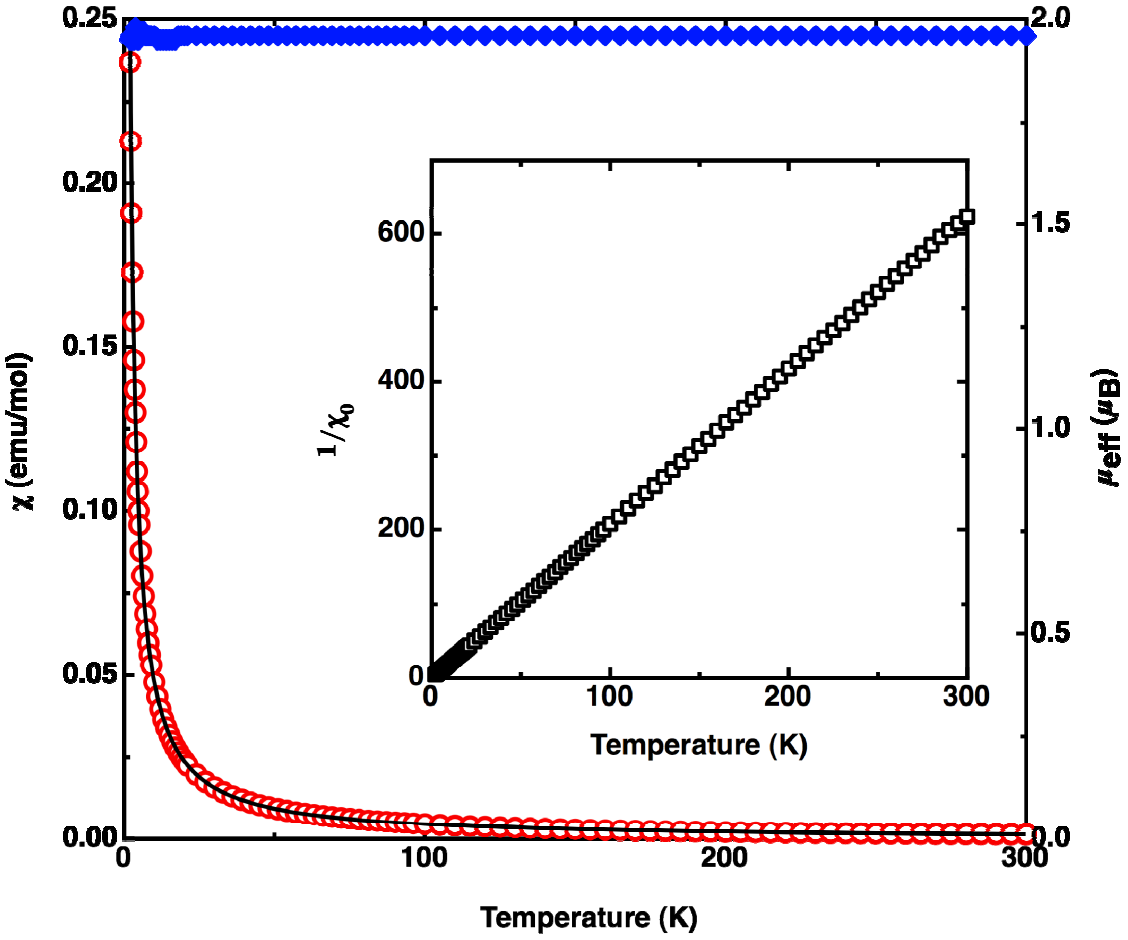

Figure S26. The temperature dependence of the magnetic susceptibility χ (red circles) and of the effective magnetic moment μ_{eff} (blue diamonds) of compound **6** in the 2-300 K temperature range. The inset shows the temperature dependence of the inverse susceptibility $1/\chi_0$.

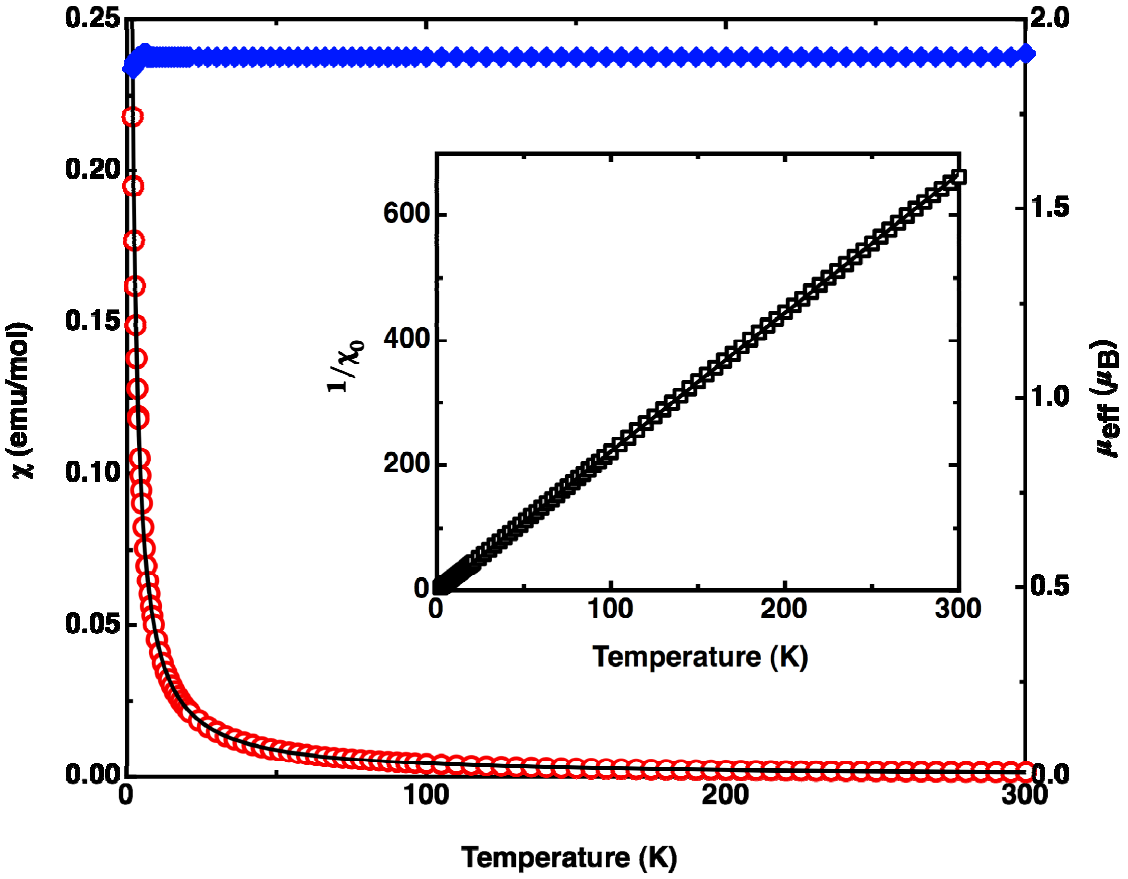

Figure S27. The temperature dependence of the magnetic susceptibility χ (red circles) and of the effective magnetic moment μ_{eff} (blue diamonds) of compound **7a** in the 2-300 K temperature range. The inset shows the temperature dependence of the inverse susceptibility $1/\chi_0$.

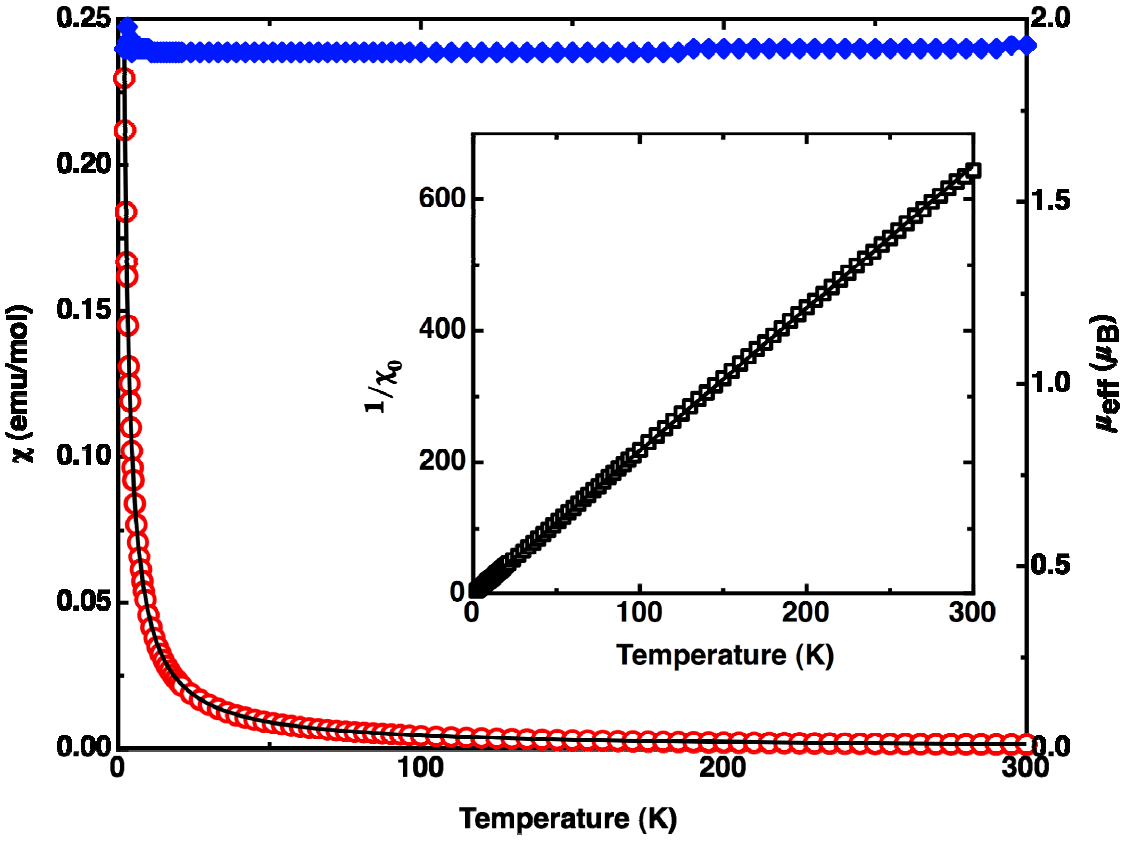

Figure S28. The temperature dependence of the magnetic susceptibility χ (red circles) and of the effective magnetic moment μ_{eff} (blue diamonds) of compound **8** in the 2-300 K temperature range. The inset shows the temperature dependence of the inverse susceptibility $1/\chi_0$.

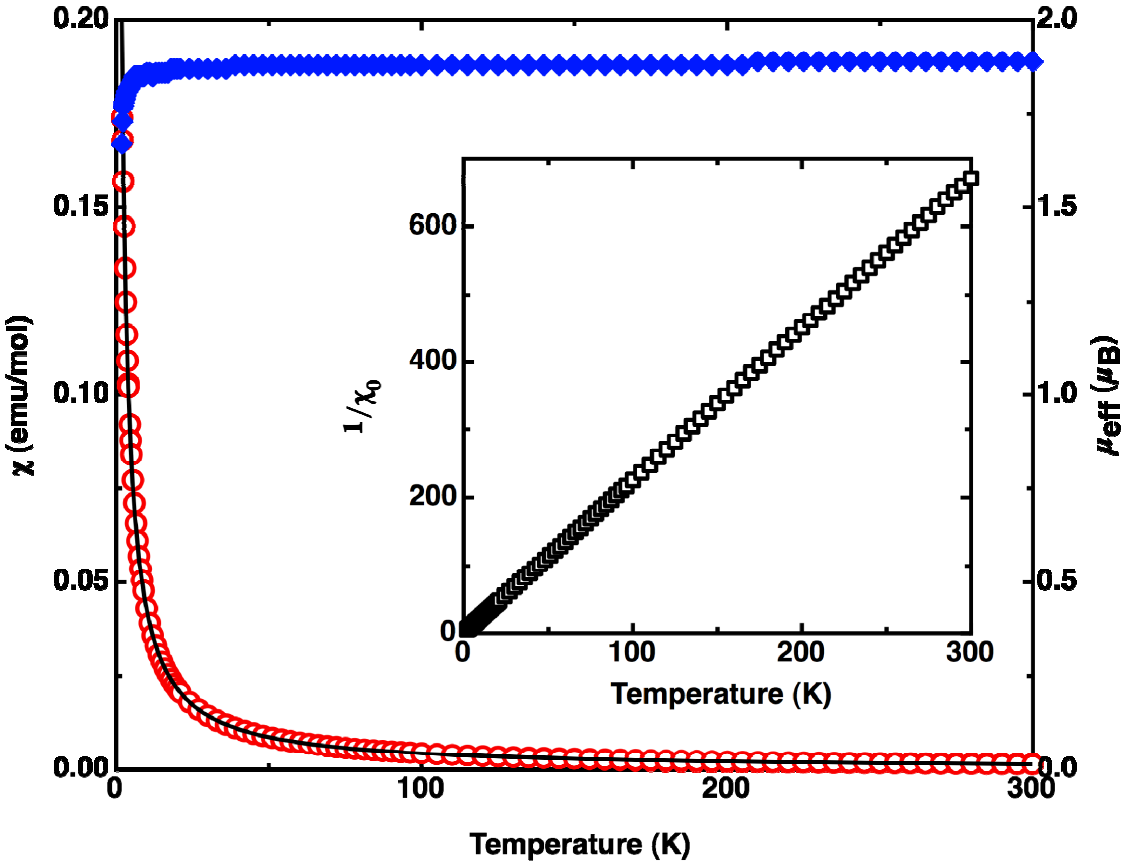

Figure S29. The temperature dependence of the magnetic susceptibility χ (red circles) and of the effective magnetic moment μ_{eff} (blue diamonds) of compound **9** in the 2-300 K temperature range. The inset shows the temperature dependence of the inverse susceptibility $1/\chi_0$.

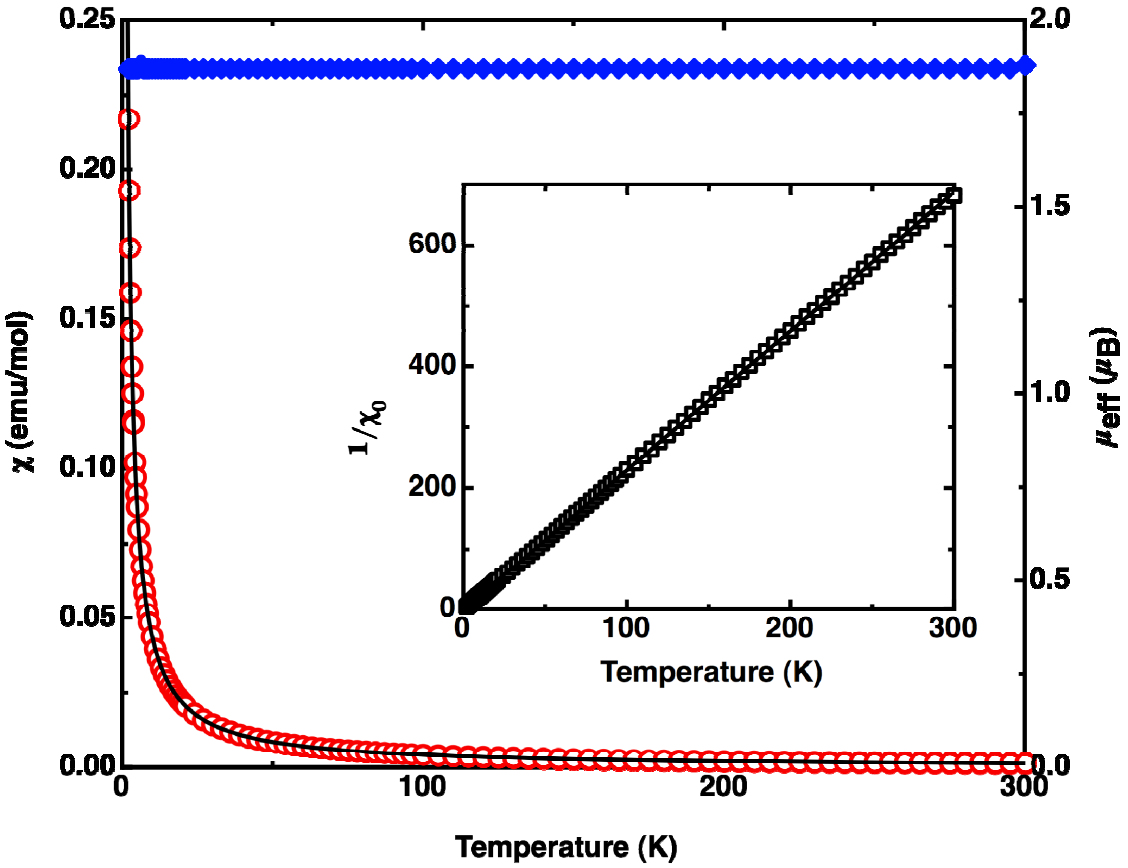

Figure S30. The temperature dependence of the magnetic susceptibility χ (red circles) and of the effective magnetic moment μ_{eff} (blue diamonds) of compound **10** in the 2-300 K temperature range. The inset shows the temperature dependence of the inverse susceptibility $1/\chi_0$.

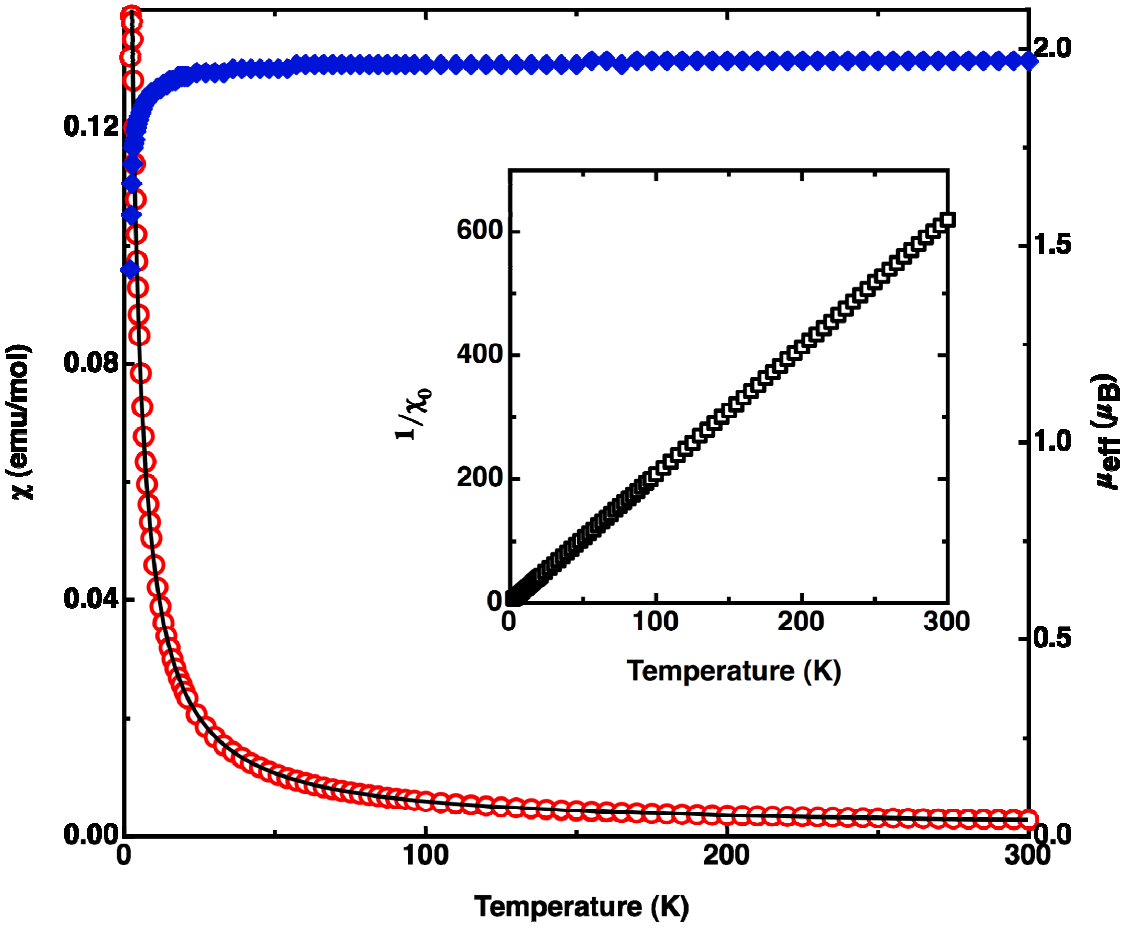

Figure S31. The temperature dependence of the magnetic susceptibility χ (red circles) and of the effective magnetic moment μ_{eff} (blue diamonds) of compound **11** in the 2-300 K temperature range. The inset shows the temperature dependence of the inverse susceptibility $1/\chi_0$.

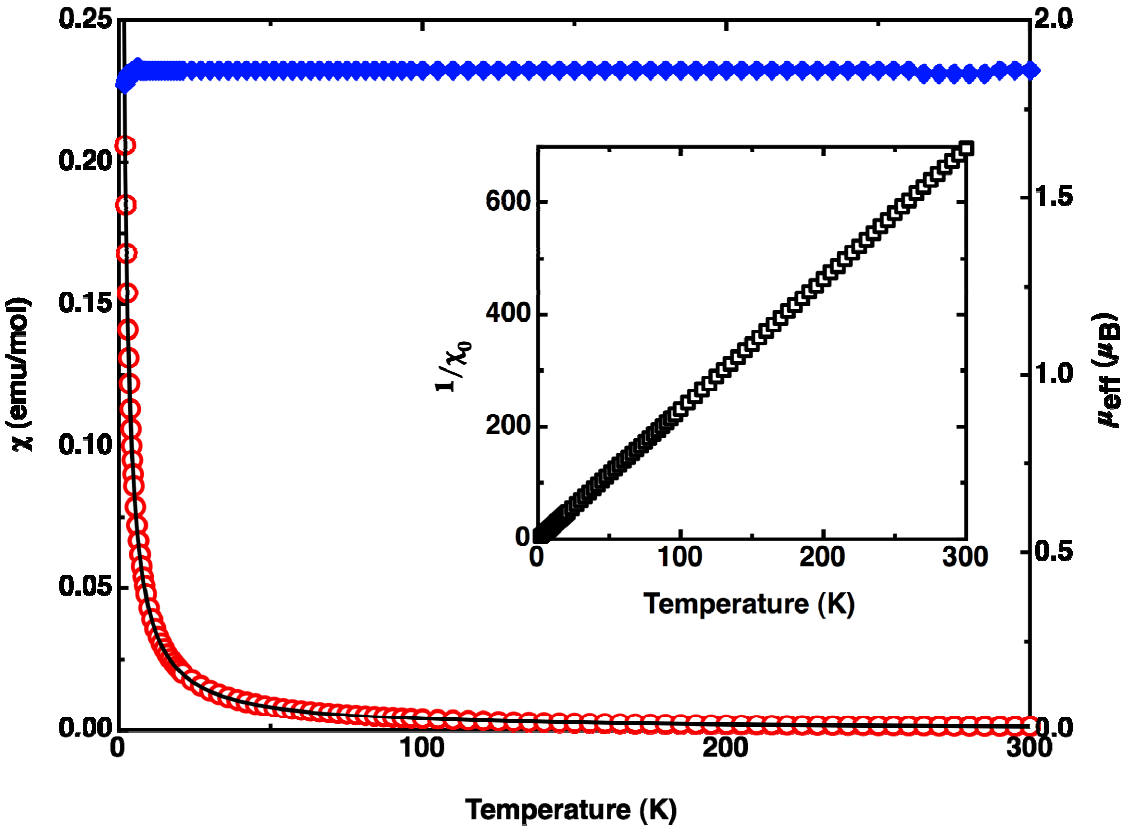

Figure S32. The temperature dependence of the magnetic susceptibility χ (red circles) and of the effective magnetic moment μ_{eff} (blue diamonds) of compound **15** in the 2-300 K temperature range. The inset shows the temperature dependence of the inverse susceptibility $1/\chi_0$.

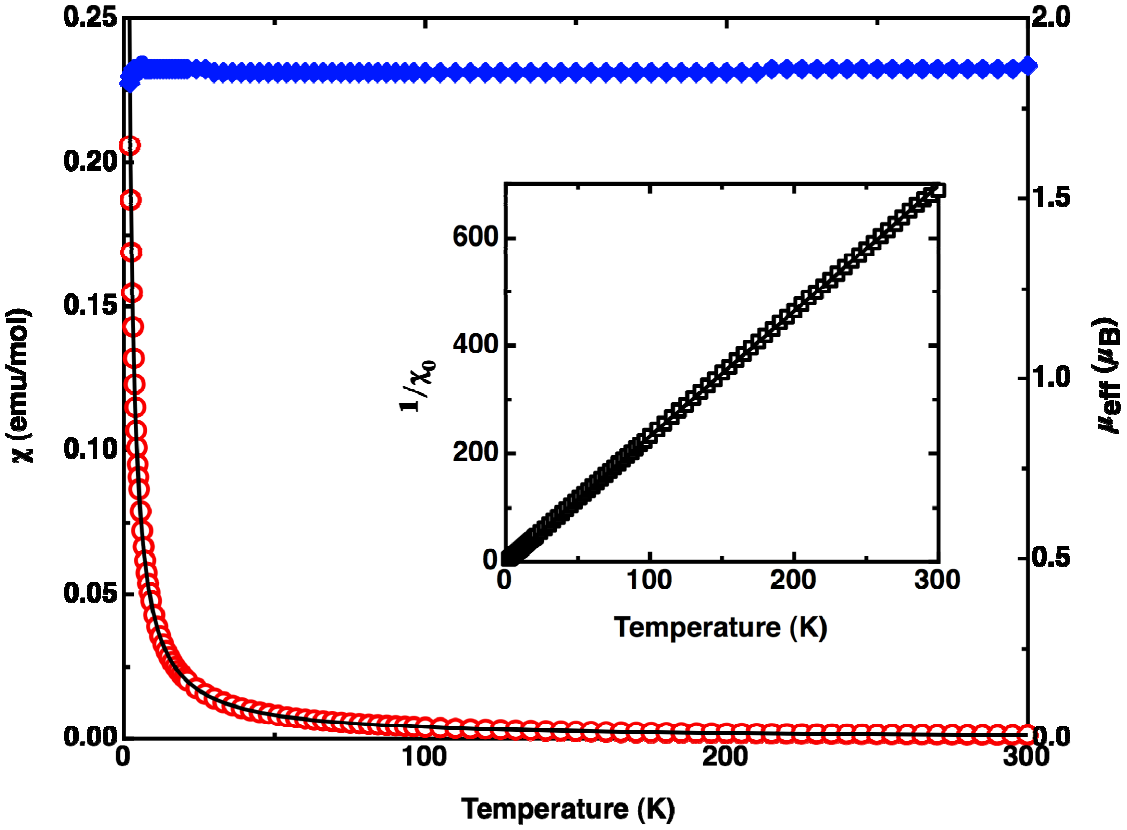

Figure S33. The temperature dependence of the magnetic susceptibility χ (red circles) and of the effective magnetic moment μ_{eff} (blue diamonds) of compound **16** in the 2-300 K temperature range. The inset shows the temperature dependence of the inverse susceptibility $1/\chi_0$.

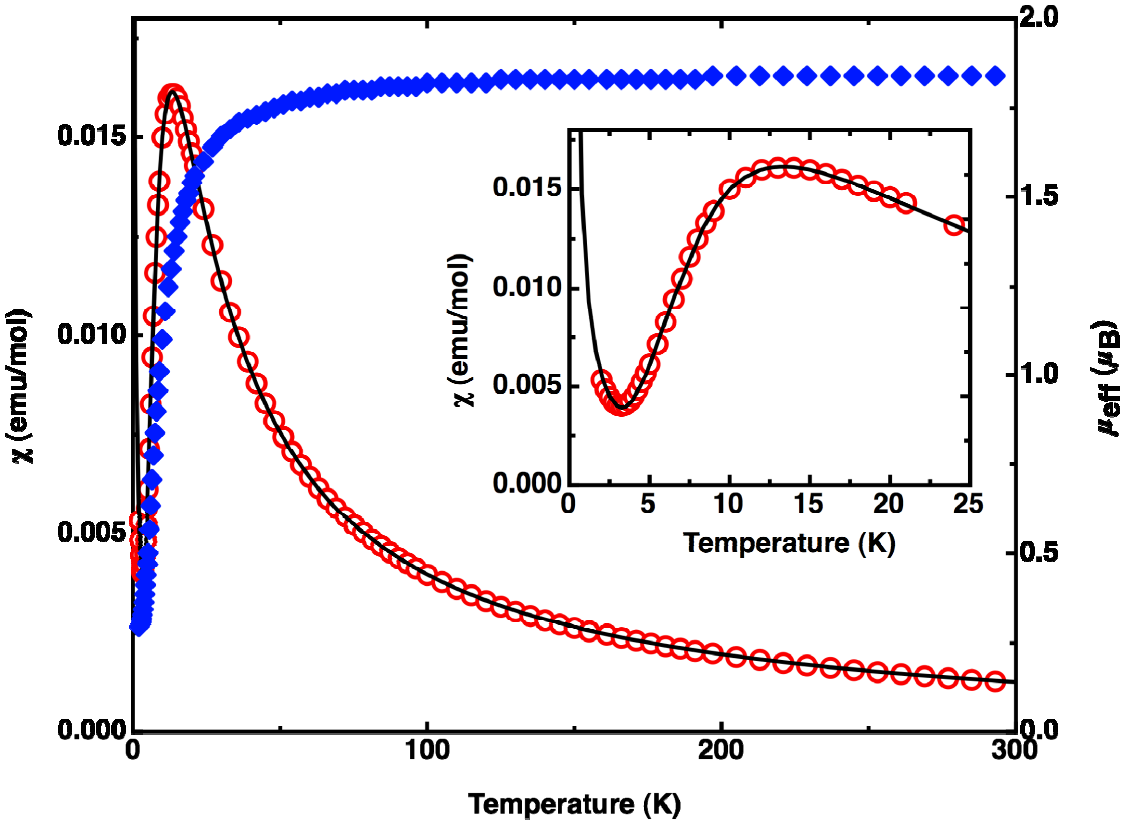

Figure S34. The temperature dependence of the magnetic susceptibility χ (red circles) and of the effective magnetic moment μ_{eff} (blue diamonds) of compound **18** in the 2-300 K temperature range. The inset shows the temperature dependence of the susceptibility χ in the 2-25 K temperature range.

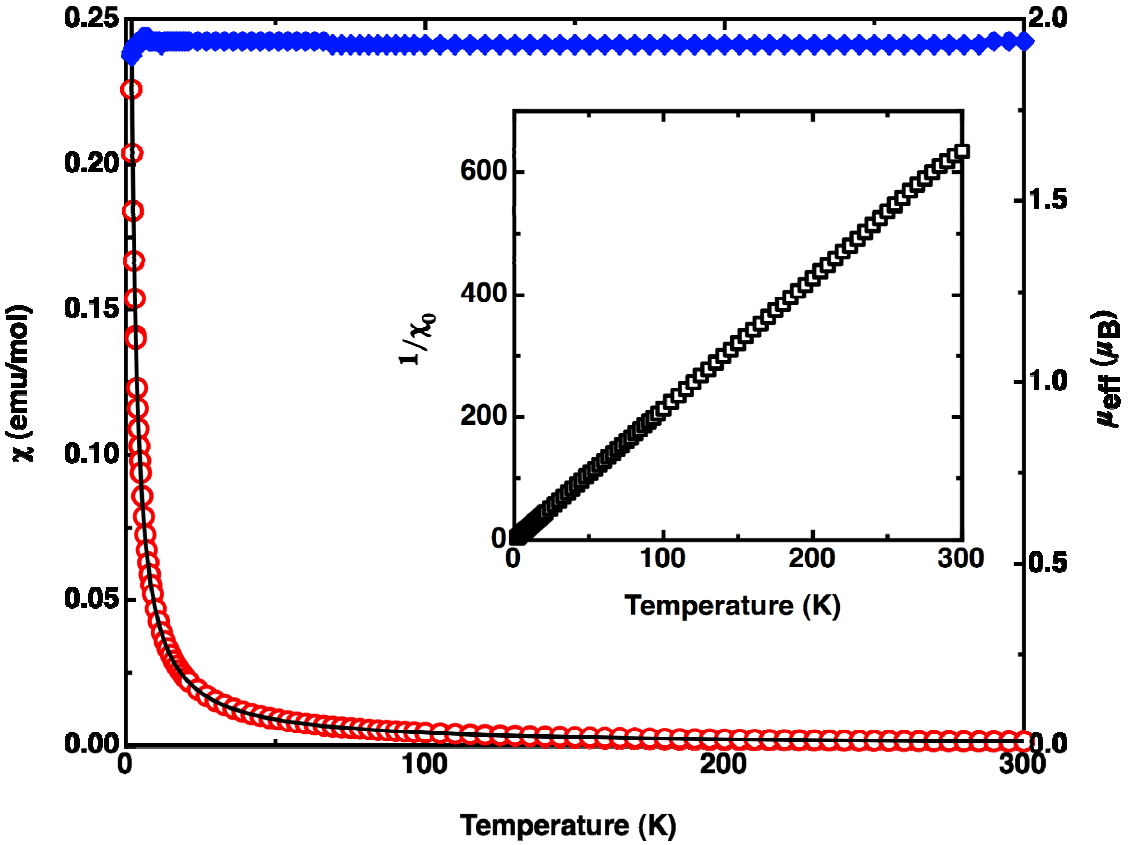

Figure S35. The temperature dependence of the magnetic susceptibility χ (red circles) and of the effective magnetic moment μ_{eff} (blue diamonds) of compound **19** in the 2-300 K temperature range. The inset shows the temperature dependence of the inverse susceptibility $1/\chi_0$.

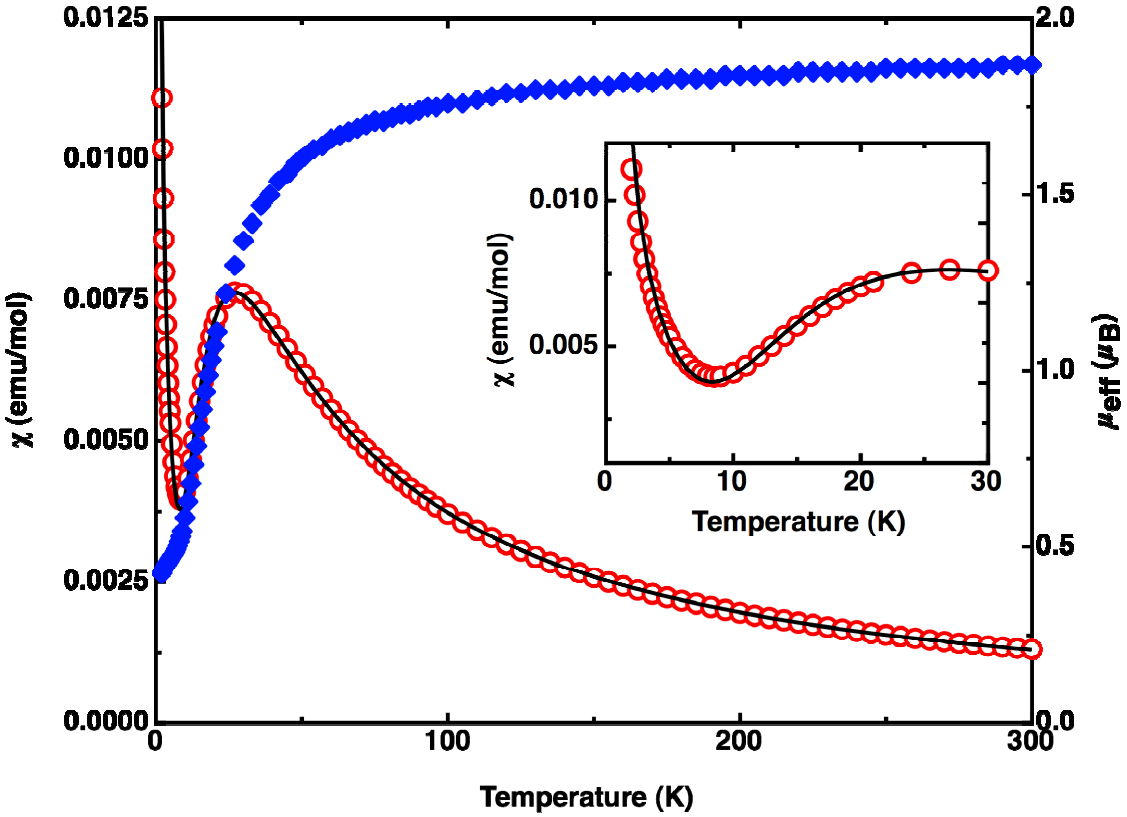

Figure S36. The temperature dependence of the magnetic susceptibility χ (red circles) and of the effective magnetic moment μ_{eff} (blue diamonds) of compound **20** in the 2-300 K temperature range. The inset shows the temperature dependence of the susceptibility χ in the 2-30 K temperature range.